INTERNATIONAL JOURNAL OF OPTIMIZATION IN CIVIL ENGINEERING
Int. J. Optim. Civil Eng., 2011; 4:609-632

OPTIMAL SHAPE DESIGN OF GRAVITY DAMS BASED ON A HYBRID META-HERURISTIC METHOD AND WEIGHTED LEAST SQUARES SUPPORT VECTOR MACHINE

J. Salajegheh[*, †,a] and S. Khosravi[b]
[a]*Department of Civil Engineering, Shahid Bahonar University of Kerman, Kerman, Iran*
[b]*College of Graduate Studies, Islamic Azad University, Kerman Branch, Kerman, Iran*

ABSTRACT

A hybrid meta-heuristic optimization method is introduced to efficiently find the optimal shape of concrete gravity dams including dam-water-foundation rock interaction subjected to earthquake loading. The hybrid meta-heuristic optimization method is based on a hybrid of gravitational search algorithm (GSA) and particle swarm optimization (PSO), which is called GSA-PSO. The operation of GSA-PSO includes three phases. In the first phase, a preliminary optimization is accomplished using GSA as local search. In the second phase, an optimal initial swarm is produced using the optimum result of GSA. Finally, PSO is employed to find the optimum design using the optimal initial swarm. In order to reduce the computational cost of dam analysis subject to earthquake loading, weighted least squares support vector machine (WLS-SVM) is employed to accurately predict dynamic responses of gravity dams. Numerical results demonstrate the high performance of the hybrid meta-heuristic optimization for optimal shape design of concrete gravity dams. The solutions obtained by GSA-PSO are compared with those of GSA and PSO. It is revealed that GSA-PSO converges to a superior solution compared to GSA and PSO, and has a lower computation cost.

Received: 5 August 2011, Accepted: 28 December 2011

KEY WORDS: Concrete gravity dams; optimal shape; gravitational search algorithm; particle swarm optimization; weighted least squares support vector machine

[*]Corresponding author: J. Salajegheh, Department of Civil Engineering, Shahid Bahonar University of Kerman, Kerman, Iran
[†]E-mail address: J.Salajegheh@mail.uk.ac.ir

1. INTRODUCTION

The economy and safety of a concrete gravity dam depend on an appropriate shape design. Hence, a proper shape design of concrete gravity dams is an important problem in dam engineering. To find a proper shape, several alternative schemes with various patterns should be selected and modified to obtain a number of feasible shapes. The proper shape of dam considering the economy and safety of design, structural considerations, etc. is selected as the final shape. In order to overcome these difficulties and achieve an optimal shape for dams, optimization techniques can be effectively utilized [1].

During the last years, various studies related to design optimization of arch dams were reported [2-9]. The optimum design of arch dams was considered under static and dynamic loads. In these studies, the effect of arch dam-water-foundation rock interaction was neglected and conventional mathematical models were utilized for analysis approximation and optimization task. In recent years, the studies on the subject of arch dam optimization have been developed. Salajegheh *et al*. [10] employed simultaneous perturbation stochastic approximation (SPSA) method with hydrodynamic effects to find optimum design. Shape optimization of arch dams using a fuzzy inference system, wavelet neural network and grading strategy is performed by Seyedpoor *et al*. [11, 12]. Akbari and Ahmadi [13] optimized real double curvature parabolic arch dam with the sequential quadratic programming (SQP) method. Akbari *et al*. [1] presented a new algorithm based on Hermit Splines with SQP method for optimal shape design of arch dams. A study was introduced by Seyedpoor *et al*. [14] so that optimal shape design of arch dams including hydrodynamic and the material nonlinearity effects is achieved using an improved particle swarm optimization (IPSO) and a wavelet back propagation (WBP) neural network.

The meta-heuristic optimization techniques in comparison with gradient-based methods have been suitable tools for global searches. In this study, the optimal shape of arch dams including dam-water-foundation rock interaction is investigated using a hybrid meta-heuristic optimization method. The hybrid meta-heuristic optimization method is based on a combination of gravitational search method (GSA) and particle swarm optimization (PSO), called GSA-PSO. The load cases involved here are gravity load, hydrostatic and hydrodynamic pressures, and earthquake load which is treated with the time history analysis of concrete gravity dam model. The weight of concrete gravity dam body is considered as the objective function. The design constraints include behavior, geometric and stability constraints. The design variables are the shape parameters of the concrete gravity dam. Due to the fact that the computational burden of optimization for time history analysis is high, weighted least squares support vector machine (WLS-SVM) is employed to predict the time history response of dams. Therefore, WLS-SVM can substantially reduce the computing effort of optimization procedure. In order to assess the efficiency of the proposed optimization method, the optimization task is performed by GSA, PSO and GSA-PSO algorithms. Numerical results show the computational advantages of the proposed meta-heuristic optimization for optimal shape design of concrete gravity dams.

2. GEOMETRICAL MODEL OF GRAVITY DAM

In order to define the geometrical model of gravity dams, the shape of gravity dams can be defined using seven parameters. According to the model shown in Figure 1, a gravity dam can be created by a vector $\boldsymbol{X}$ that has seven components including shape parameters of the concrete gravity dam as:

$$\mathrm{X} = \{b \quad b_1 \quad b_2 \quad b_3 \quad H_2 \quad H_4 \quad H_5\} \tag{1}$$

where b and H_1 are two parameters required to defined crest and free board of gravity dam, respectively. H_3 depends on H_4 and reservoir water level (H). The shape parameters of the gravity dam are shown in Figure 1.

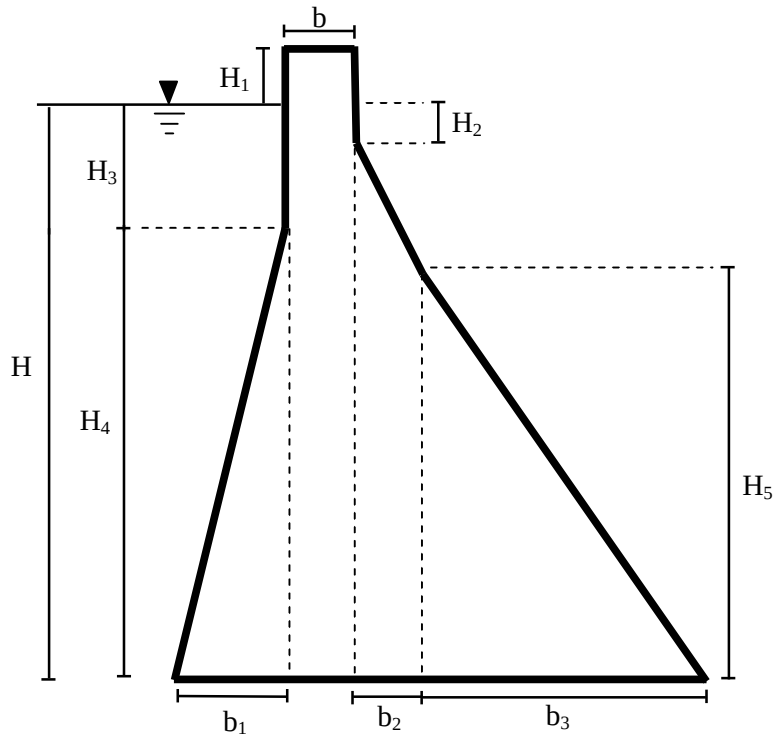

Figure 1. Geometrical model of gravity dam.

3. FINITE ELEMENT MODEL OF GRAVITY DAM-WATER-FOUNDATION ROCK SYSTEM

In solving the fluid-structure interaction problem using finite element method (FEM), the discretized dynamic equations of the fluid and structure need to be considered simultaneously to obtain the coupled fluid-structure equation.

3.1. Structural responses

The solid dam is discretized by using finite elements and its equations of seismic motion including the effects of the reservoir and the foundation are expressed as [15]:

$$\boldsymbol{M}_s \ddot{\boldsymbol{u}}_e + \boldsymbol{C}_s \dot{\boldsymbol{u}}_e + \boldsymbol{K}_s \boldsymbol{u}_e = -\boldsymbol{M}_s \ddot{\boldsymbol{u}}_g + \boldsymbol{Q}\boldsymbol{p}_e \tag{2}$$

where $\boldsymbol{M}_s$ is the structural mass matrix, $\boldsymbol{C}_s$ is the structural damping matrix, $\boldsymbol{K}_s$ is the structural stiffness matrix, $\boldsymbol{u}_e$ is the vector of the nodal displacements relative to the ground, $\ddot{\boldsymbol{u}}_g$ is the vector of the ground acceleration, $\boldsymbol{Q}\boldsymbol{p}_e$ represents the nodal force vector associated with the hydrodynamic pressures produced by the reservoir.

The structural damping in the system is usually included by using a Rayleigh type of damping matrix given by [15]:

$$C_S = \bar{a}\, \boldsymbol{M}_S + \bar{b}\, \boldsymbol{K}_S \tag{3}$$

where $\bar{a}$ and $\bar{b}$ are constants adjusted to obtain a desirable damping in the system, usually on the basis of given modal damping ratios.

3.2. Reservoir responses

For a compressible and inviscid fluid, the hydrodynamic pressure p resulting from the ground motion of the rigid dam (Figure 2) satisfies the wave equation in the form [16, 17]:

$$\nabla^2 p = \frac{1}{c^2} \frac{\partial^2 p}{\partial t^2} \tag{4}$$

where c is the velocity of sound in water and ∇^2 is the Laplacian operator in two dimensions.

The following boundary conditions are defined by assuming that the effects of surface waves and the viscosity of the fluid are neglected. As shown in Figure 2, some boundary conditions may be imposed on the fluid domain as follows:

i) At the fluid-solid interface (S1),

$$\frac{\partial p}{\partial n} = -r_w\, a_n \tag{5}$$

where n is the unit normal vector, a_n is the normal acceleration on the interface and r is the mass density of the fluid.

ii) At the bottom of the fluid domain (S2),

$$\frac{\partial p}{\partial n} = -r\, a_n - \bar{q} \frac{\partial p}{\partial t} \tag{6}$$

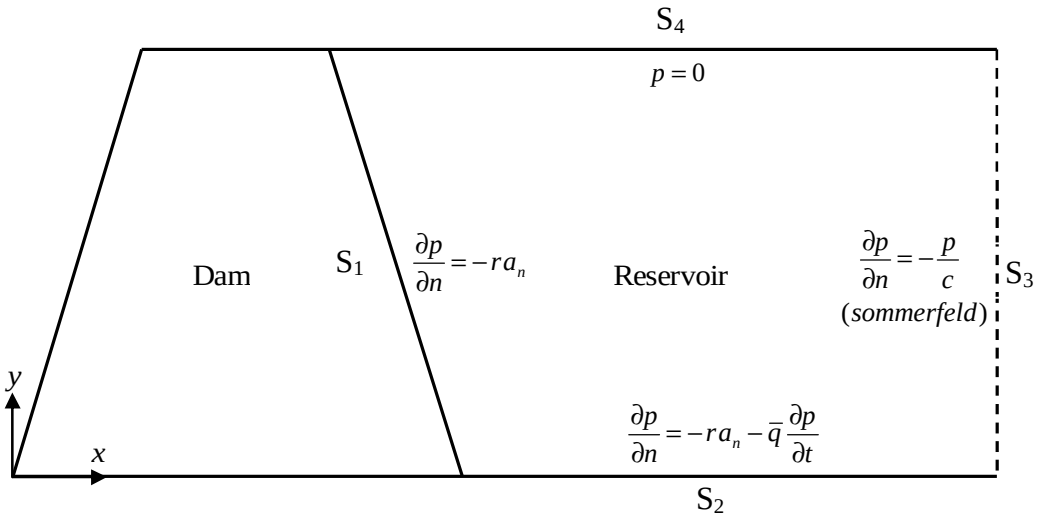

Figure 2. The boundary conditions of the fluid domain [17]

where $\bar{q}$ is a damping coefficient which is the fundamental parameter characterizing the effects of the reservoir bottom materials. Relation between damping coefficient and ratio of reflected hydrodynamic pressure wave, a , is [18]:

$$a = \frac{1-\bar{q}c}{1+\bar{q}c} \tag{7}$$

iii) At the far end (S3); A Sommerfeld-type radiation boundary condition can be implemented, namely:

$$\frac{\partial p}{\partial n} = -\frac{\dot{p}}{c} \tag{8}$$

iv) At the free surface (S4),

$$p = 0 \tag{9}$$

Eqs. (4)-(9) can be discretized to get the matrix form of the wave equation as [16, 17]:

$$\boldsymbol{M}_f \ddot{\boldsymbol{p}}_e + \boldsymbol{C}_f \dot{\boldsymbol{p}}_e + \boldsymbol{K}_f \boldsymbol{p}_e + r_w \boldsymbol{Q}^T (\ddot{\boldsymbol{u}}_e + \ddot{\boldsymbol{u}}_g) = 0 \tag{10}$$

where $\boldsymbol{M}_f$, $\boldsymbol{C}_f$ and $\boldsymbol{K}_f$ are the fluid mass, damping and stiffness matrices, respectively, and $\boldsymbol{p}_e$ and $\ddot{\boldsymbol{u}}_e$ are the nodal pressure and relative nodal acceleration vectors, respectively. The term $r_w \boldsymbol{Q}^T$ is also often referred to as coupling matrix.

3.3. The coupled fluid-structure equation

Eqs. (2) and (10) describe the complete finite-element discretized equations for the gravity

dam-water-foundation rock interaction problem and can be written in an assembled form as [16, 17]:

$$\begin{bmatrix} \boldsymbol{M}_s & 0 \\ \boldsymbol{M}_{fs} & \boldsymbol{M}_f \end{bmatrix} \begin{Bmatrix} \ddot{\boldsymbol{u}}_e \\ \ddot{\boldsymbol{p}}_e \end{Bmatrix} + \begin{bmatrix} \boldsymbol{C}_s & 0 \\ 0 & \boldsymbol{C}_f \end{bmatrix} \begin{Bmatrix} \dot{\boldsymbol{u}}_e \\ \dot{\boldsymbol{p}}_e \end{Bmatrix} + \begin{bmatrix} \boldsymbol{K}_s & \boldsymbol{K}_{fs} \\ 0 & \boldsymbol{K}_f \end{bmatrix} \begin{Bmatrix} \boldsymbol{u}_e \\ \boldsymbol{p}_e \end{Bmatrix} = \begin{Bmatrix} -\boldsymbol{M}_s \ddot{\boldsymbol{u}}_g \\ -\boldsymbol{M}_{fs} \ddot{\boldsymbol{u}}_g \end{Bmatrix} \tag{11}$$

where $\boldsymbol{M}_{fs} = r_w \boldsymbol{Q}^T$ *and* $\boldsymbol{K}_{fs} = -\boldsymbol{Q}$. Eq. (11) expresses a second order linear differential equation having unsymmetrical matrices and may be solved by means of direct integration methods.

In the present study, the finite-element idealization of gravity dam-water-foundation rock system is implemented on the mentioned theory and assumptions. The gravity dam is treated as a two-dimensional-linear structure. The four-noded solid element is utilized to mesh the dam body. The four-noded fluid element is used to discretize the fluid medium and the interface of the fluid-structure interaction problem. The element has four degrees of freedom per node: translations in the nodal *x*, *y* and *x* directions and pressure. The translations are applicable only at nodes that are on the interface. In the fluid-structure interaction problem, the damping matrix of the fluid domain is produced by applying a boundary condition to the bottom, sides and far-end of the reservoir. A Sommerfield-type radiation boundary condition is used at the far-end boundary of the reservoir. Interaction between the fluid and foundation rock is considered through a damping boundary condition applied along the bottom and sides of the reservoir defined by the second term of Eq. (6). The damping matrix of the dam is also accomplished using the Rayleigh damping taken into account by Eq. (3). In this study, foundation rock treating as a linearly elastic structure is represented via a four-noded solid element as well. The foundation rock is assumed to be massless in which only the effects of foundation flexibility are considered and the inertia and damping effects of the foundation rock are neglected. The foundation rock is extended to 1.5 times base width of dam. In the analysis phase, a static analysis of the gravity dam-water-foundation rock system is initially implemented under a gravity load and a hydrostatic pressure and then, the linear dynamic analysis of the system is performed using the Newmark time integration method [15]. After that, nodal relative displacement vector of the structure is utilized to evaluate the principal stresses at the center of dam elements via conventional FEM.

4. GRAVITY DAM OPTIMIZATION PROBLEM

The gravity dam optimization problem subjected to earthquake loading is stated as follows:

$$\begin{aligned} &\text{Minimize} \quad f(\boldsymbol{X}) \\ &\text{Subject to} \quad g_j(\boldsymbol{X},t) \le 0 \quad j = 1,2,\ldots,m \\ &\qquad\qquad \boldsymbol{X}^L \le \boldsymbol{X} \le \boldsymbol{X}^U \end{aligned} \tag{12}$$

where *f*, g_j and t are the objective function, the constraints and the time. $\boldsymbol{X}^L$ and $\boldsymbol{X}^U$ are the

lower bound and the upper bound of the design variables, $\boldsymbol{X}$.

According to the geometrical model of the gravity dam described in Section 2, the design variable vector can be adopted from Eq. (1). In the optimization problem, $f(\boldsymbol{X})$ represents the concrete weight of a gravity dam body that should be minimized. The concrete weight can be determined by:

$$f(\boldsymbol{X}) = W = r_c\, gV \tag{13}$$

where r_c and V are mass density and volume of gravity dam, respectively. g is gravity acceleration.

Also, in Eq. (12) $g_j(\boldsymbol{X},t)$ are inequality constraints that may be categorized into the behavior, geometric and stability constraints. The behavior constraints dependent on time. In this study, the principal stresses of each node for the gravity dam is considered as the behavior constraints, which must be satisfied for all time points of the earthquake interval. These constraints are expressed as follows:

$$g_{k,1} = \frac{s_1(\boldsymbol{X},t)}{s^+} - 1 \qquad k = 1,2,...,nj \tag{14}$$

$$g_{k,2} = \frac{\left|s_2(\boldsymbol{X},t)\right|}{s^-} - 1 \qquad k = 1,2,...,nj \tag{15}$$

where $s_1(\cdot)$ and $s_2(\cdot)$ are the principal stresses of each node in time *t*, respectively. s^+ and s^- are the allowable tensional and compressive stresses. *nj* is the total number of dam nodes which created by meshing of the dam body.

The stability of a dam is ordinarily expressed in terms of its factors of safety against sliding and overturning, respectively. The factor of safety against sliding is simply the ratio of the total frictional force, F_V, which the foundation can develop to the force tending, F_H, to cause sliding. The constraint can be expressed as follows [19]:

$$g_s = \frac{\sum F_V}{\sum F_H} - 1.75 \tag{16}$$

The factor of safety against overturning about the toe is the ratio of the resisting moments, M_R, to the overturning moments, M_O, which is considered as stability constraint. It is given as [19]:

$$g_o = \frac{\sum M_R}{\sum M_O} - 1 \tag{17}$$

A number of constraint-handling techniques have been proposed to solve constrained

optimization problems. In this study, the penalty function is used to deal with constrained search spaces as:

$$fit(\boldsymbol{X}) = \begin{cases} f(\boldsymbol{X}) & \text{if } \boldsymbol{X} \in R^d \\ f(\boldsymbol{X})(1 + r_p\, G(\boldsymbol{X},t)) & \text{otherwise} \end{cases} \tag{18}$$

where $fit(\boldsymbol{X})$ and r_p is modified function (fitness function) and an adjusting coefficient; R^d denotes the feasible search space; and $G(\boldsymbol{X},t)$ is the penalization factor, which is defined as the sum of all active constraints violations; as indicated:

$$G(\boldsymbol{X},t) = \sum_{t=0}^{T} \sum_{k=1}^{nj} \left[\max(g_{k,1},0)^2 + \max(g_{k,2},0)^2 \right] + \max(g_s,0)^2 + \max(g_o,0)^2 \tag{19}$$

This formulation allows that for solutions with violated constraints, the objective function is always greater than the non-violated one.

5. OPTIMIZATION METHOD

In the present study, to find the optimal shapes of gravity dams a hybrid meta-heuristic optimization algorithm is presented. This meta-heuristic optimization algorithm is based on a combination of gravitational search method (GSA) and particle swarm optimization (PSO), called GSA-PSO. In this section PSO and GSA algorithms are described at first, and then the proposed GSA-PSO is introduced.

5.1. Particle swarm optimization

Recently, in structural engineering the successful applications of PSO as an optimization engine have been reported by Refs. [20-26]. PSO has been inspired by the social behavior of animals such as fish schooling, insects swarming and birds flocking. The PSO algorithm is introduced by Kennedy and Eberhart [27] in the mid 1990s, while attempting to simulate the graceful motion of bird swarms as a part of a socio-cognitive study. It involves a number of particles, which are initialized randomly in the search space of an objective function. These particles are referred to as swarm. Each particle of the swarm represents a potential solution of the optimization problem. The *i*th particle in *l*th iteration is associated with a position vector, $\boldsymbol{X}_i^l$, and a velocity vector, $\boldsymbol{V}_i^l$, that shown as following,

$$\begin{aligned} \boldsymbol{X}_i^l &= \{ x_{i1}^l, x_{i2}^l, \ldots, x_{iD}^l \} \\ \boldsymbol{V}_i^l &= \{ v_{i1}^l, v_{i2}^l, \ldots, v_{iD}^l \} \end{aligned} \tag{20}$$

where *D* is dimension of the solution space.

The particle fly through the solution space and its position is updated based on its velocity, the best position particle (***pbest***) and the global best position (***gbest***) that swarm has visited

since the first iteration as,

$$\boldsymbol{V}_i^{l+1} = w^l \boldsymbol{V}_i^l + c_1 r_1 (\boldsymbol{pbest}_i^l - \boldsymbol{X}_i^l) + c_2 r_2 (\boldsymbol{gbest}^l - \boldsymbol{X}_i^l) \tag{21}$$

$$\boldsymbol{X}_i^{l+1} = \boldsymbol{X}_i^l + \boldsymbol{V}_i^{l+1} \tag{22}$$

where r_1 and r_2 are two uniform random sequences generated from interval [0, 1]; c_1 and c_2 are the cognitive and social scaling parameters, respectively and w^l is the inertia weight used to discount the previous velocity of particle preserved.

Shi and Eberhart [28] proposed that the cognitive and social scaling parameters c_1 and c_2 to be selected such that c_1=c_2=2 to allow the product c_1r_1 or c_2r_2 to have a mean of 1. One of the main parameters affecting the performance of PSO is the inertia weight (w) in achieving efficient search behavior. A dynamic variation of inertia weight is proposed by linearly decreasing w with each iteration algorithm as shown in Eq. (23) [28],

$$w = w_{\max} - \frac{w_{\max} - w_{\min}}{l_{\max}} l \tag{23}$$

where $w_{\max}$ and $w_{\min}$ are the maximum and minimum values of ω , respectively. Also, l_{max} is the numbers of maximum iteration.

5.2. Gravitational search algorithm

The gravitational search algorithm (GSA) was first introduced by Rashedi *et al.* [29] as a new stochastic population-based heuristic optimization method. This approach provides an iterative method that simulates mass interactions, and moves through a multi-dimensional search space under the influence of gravitation. This heuristic algorithm has been inspired by the Newtonian laws of gravity and motion. In GSA, agents are considered as objects and their performance are measured by their masses, and all these objects attract each other by the gravity force, while this force causes a global movement of all objects towards the objects with heavier masses.

In GSA, each agent of the population represents a potential solution of the optimization problem. The *i*th agent in *l*th iteration is associated with a position vector, $\boldsymbol{X}_i(l)$, and a velocity vector, $\boldsymbol{V}_i(l)$, that shown as following:

$$\begin{aligned} \boldsymbol{X}_i(l) &= \{ x_i^1, x_i^2, ..., x_i^D \} \\ \boldsymbol{V}_i(l) &= \{ v_i^1, v_i^2, ..., v_i^D \} \end{aligned} \tag{24}$$

The mass of each agent is calculated after computing the current population fitness for a minimization problem, as follows [29]:

$$q_i(l) = \frac{fit_i(l) - worst(l)}{best(l) - worst(l)} \tag{25}$$

$$M_i(l) = \frac{q_i(l)}{\sum_{j=1}^{N} q_i(l)} \tag{26}$$

where N, $M_i(l)$ and $fit_i(l)$ represent the population size, the mass and the fitness value of agent i at $l$the iteration, and $worst(l)$ and $best(l)$ are defined as follows:

$$best(l) = \min\{ fit_1(l), fit_2(l), ..., fit_N(l)\} \tag{27}$$

$$worst(l) = \max\{ fit_1(l), fit_2(l), ..., fit_N(l)\} \tag{28}$$

To compute the acceleration of an agent, total forces from a set of heavier masses applied on it should be considered based on a combination of the law of gravity and the second law of Newton on motion (Eq. (29)) [29]. Afterwards, the next velocity of an agent is calculated as a fraction of its current velocity added to its acceleration (Eq. (30)). Then, its position could be calculated using Eq. (31).

$$a_i^d(l) = \sum_{j \in kbest,\, j \neq i} rand_j G(l) \frac{M_j(l)}{R_{ij}(l) + e} (x_j^d(l) - x_i^d(l)) \tag{29}$$

$$v_i^d(l+1) = rand_i v_i^d(l) + a_i^d(l) \tag{30}$$

$$x_i^d(l+1) = x_i^d(l) + v_i^d(l+1) \tag{31}$$

where a_i^d, v_i^d and x_i^d present the acceleration, velocity and position of ith agent in dimension d, respectively. $rand_i$ and $rand_j$ are two uniform random numbers in the interval [0, 1]; e is a small value; n is the dimension of the search space; and $R_{ij}(l)$ is the Euclidean distance between agent i and j. *kbest* is the set of first K agents with the best fitness value and biggest mass, which is a function of time, initialized to K_0 at the beginning and decreased with time. G is a decreasing function of time. In this study, $G(l)$ is considered as a linear decreasing function in the GSA algorithm as follows:

$$G(l) = G_0 (1 - \frac{l}{l_{\max}}) \tag{32}$$

This function is set to G_0 at the beginning and decreases exponentially towards zero with lapse of time.

5.3. The hybrid of GSA-PSO method

The PSO algorithm is one of the most proficient meta-heuristic techniques which is an algorithm inspired by the social behavior of flock populations. In structural engineering the shortcoming of the PSO algorithm is to need a great number of function evaluations (structural analyses) for finding the global solution. It is expected that this drawback can be dealt with selecting an adequate initial swarm. In this study, the GSA algorithm as local search finds an optimal initial swarm for commencing the PSO algorithm. In the first stage of the GSA-PSO method, a preliminary optimization is performed by employing the GSA algorithm. The optimum design found by GSA, $\boldsymbol{X}_{\mathrm{GSA}}$, is copied N_{GSA} times to create the some part of the optimal initial swarm in the second stage. Other particles of the initial swarm, i.e. $\boldsymbol{X}_{rnd,j}\,(j=1,2,...,N_{PSO}-N_{GSA})$, are selected randomly to complete the initial swarm. Finally, PSO is employed to find a more accurate optimum design using the optimal initial swarm. The algorithm flow of GSA-PSO strategy is shown in Figure 3.

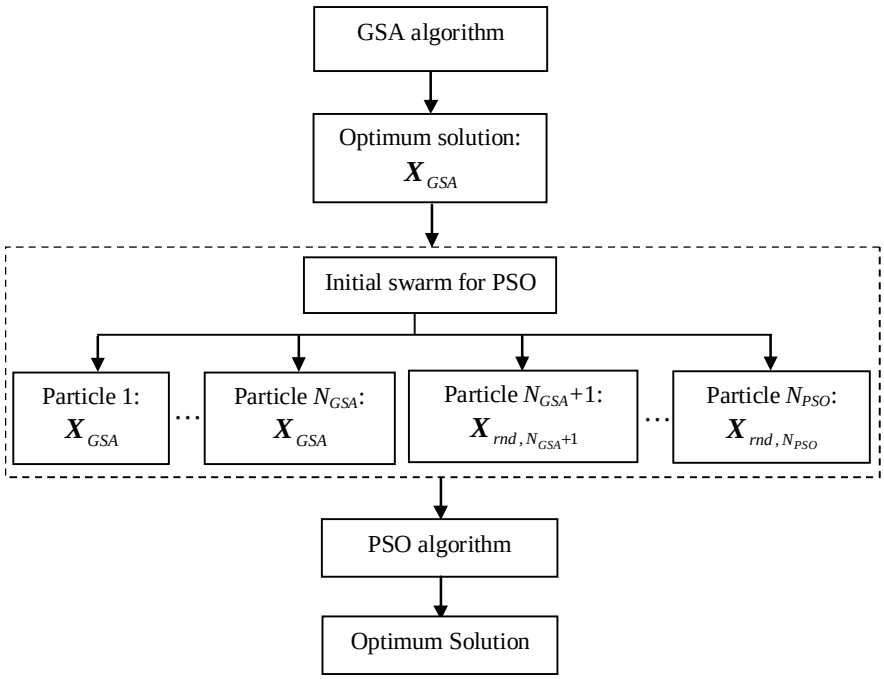

Figure 3. The algorithm flow of GSA-PSO

6. PREDICTING THE STRUCTURAL RESPONSES USING WLS-SVM

Recently, support vector machines (SVMs) have been successfully used as an excellent machine learning algorithm [30]. The SVM is developed based on the structural risk

minimization (SRM), which can escape from several drawbacks, such as local minimum and the necessity of a large number of controlling parameters in artificial neural networks (ANNs). The weighted least squares support vector machines (WLS-SVM) is introduced by Suykens *et al*. [30] to decrease the training computational effort of SVM in the large-scale problem. Further, WLS-SVM predicts functions more robust and precise by assigning weights and performance generality of WLS-SVM is better than that of least squares version of SVM (LSSVM) [30, 31]. WLS-SVM is described as the following optimization problem in primal weight space [30]:

$$\min J(\boldsymbol{w},\boldsymbol{e}) = \frac{1}{2}\|\boldsymbol{w}\|^2 + \frac{1}{2}g\sum_{i=1}^{n}\bar{v}_i e_i^2 \tag{33}$$

subject to the following equality constraints:

$$y_i = \boldsymbol{w}^T j(\boldsymbol{x}_i) + b + e_i, \qquad i = 1,2,...,n \tag{34}$$

with $\{\boldsymbol{x}_i, y_i\}_{i=1}^{n}$ a training data set, input data $\boldsymbol{x_i} \in R^n$ and output data $y_i \in R$. $j(.): R^n \to R^d$ is a function which maps the input space into a higher dimensional space. The vector $\boldsymbol{w} \in R^d$ represents weight vector in primal weight space. The symbols $e_i \in R$ and $b \in R$ represent error variable and bias term, respectively. By the optimization problem (33) and the training set, the model of WLS-SVM is defined as follows:

$$y(\boldsymbol{x}) = \boldsymbol{w}^T j(\boldsymbol{x}) + b \tag{35}$$

It is impossible to indirectly calculate $\boldsymbol{w}$ from (33), because of the structure of the function $j(\boldsymbol{x})$ is unknown in general. Therefore, the dual problem shown in Eq. (33) is minimized by the Lagrange multiplier method as follows:

$$L(\boldsymbol{w},b,\boldsymbol{e};\boldsymbol{x}) = J(\boldsymbol{w},\boldsymbol{e}) - \sum_{i=1}^{n} a_i(\boldsymbol{w}^T j(\boldsymbol{x}_i) + b + e_i - y_i) \tag{36}$$

According to the Karush-Khun-Tucker (KKT) conditions, eliminating $\boldsymbol{w}$ and $\boldsymbol{e}$ the solution is given by the following set of linear equation:

$$\begin{bmatrix} \Omega + \boldsymbol{V}_g & \boldsymbol{1}_n^T \\ \boldsymbol{1}_n & \boldsymbol{0} \end{bmatrix} \begin{bmatrix} \boldsymbol{\alpha} \\ b \end{bmatrix} = \begin{bmatrix} \boldsymbol{y} \\ 0 \end{bmatrix} \tag{37}$$

where

$$\begin{gathered} \boldsymbol{V}_g = diag\{1/g\bar{v}_1,...,1/g\bar{v}_n\} \;;\; W_{i,j} = \left\langle j(\boldsymbol{x}_i), j(\boldsymbol{x}_j)\right\rangle_H \quad i,j = 1,...,n \\ \boldsymbol{y} = [y_1,...,y_n]^T;\; \boldsymbol{1}_n^T = [1,...,1] \;;\; \boldsymbol{\alpha} = [a_1,...,a_n] \end{gathered} \tag{38}$$

According to Mercer's condition, a kernel $K(.,.)$ is selected, such that:

$$K(\boldsymbol{x}, \bar{\boldsymbol{x}}) = \langle j(\boldsymbol{x}), j(\bar{\boldsymbol{x}}) \rangle_H \tag{39}$$

So, the resulting WLS-SVM model for the prediction of functions becomes:

$$y(\boldsymbol{x}) = \sum_{i=1}^{n} a_i K(\boldsymbol{x}_i, \boldsymbol{x}) + b \tag{40}$$

Weight $\bar{v}_k$ is estimated as follows [32, 33]:

$$\bar{v}_k = \begin{cases} 1 & if \ \left| e_i / \hat{s} \right| \le c_1 \\ \dfrac{c_2 - \left| e_i / \hat{s} \right|}{c_2 - c_1} & if \ c_1 < \left| e_i / \hat{s} \right| \le c_2 \\ 10^{-4} & otherwise \end{cases} \tag{41}$$

where $\hat{s}$ is a robust estimate of the standard deviation of the error variables ($e_i = a_i / D_{ii}^{-1}$), and the constants c_1 and c_2 are typically chosen as $c_1 = 2.5$ and $c_2 = 3$ [33]. Here D_{ii}^{-1} denotes the *i*th primal diagonal element in the inversion of matrix ***D*** which is the matrix on the left-hand of the system of the linear Eq. (37) [34]. After weights $\bar{v}_k$ are determined, the model (40) is achieved by solving the WLS-SVM problem (Eq. (39)).

In this study, radial basis function (RBF) is selected as the kernel function of WLS-SVM. The kernel function is defined as follows:

$$K(\boldsymbol{x}_i, \boldsymbol{x}_j) = \exp\left(-\frac{\left\| \boldsymbol{x}_i - \boldsymbol{x}_j \right\|^2}{2 s^2}\right) \tag{42}$$

where s is positive real constant, and is usually so-called kernel width.

7. TEST EXAMPLE

In order to investigate the computational efficiency of the hybrid meta-heuristic optimization method for the shape optimization of concrete gravity dams, Pine flat dam is considered as a real-world structure. This dam located on King's River near Fresno, California. The dam structure is 400 *ft* height with a crest length of 1840 *ft* and its construction about 9491.94 *kip* concrete. The detailed properties of the dam-water system have been provided in Refs. [35, 36]. The properties of concrete, water and foundation are shown in Table 1.

Table 1. The properties of materials

Material	Property	Value
Concrete	Modulus of elasticity	3.25×10^6 psi
	Poisson's ratio	0.2
	Mass density	155 lb/ft^3
Water	Mass density	62.4 lb/ft^3
	Wave velocity	4720 ft/sec
	Wave reflection coefficient	0.817
Foundation	Modulus of elasticity	10^7 psi
	Poisson's ratio	0.33
	Mass density	0

The ground motion recorded at Taft Lincoln School Tunnel during Kern country, California, earthquake of July 21, 1952, is selected as the excitation for analyses of Pine Flat dam [35, 36]. The ground motion acting transverse to the axis of the dam is defined by the S69E component of the recorded motion. This component of the recorded ground motion is shown in Figure 4.

In the present study, to create the gravity dam geometry, seven design variables are considered. The lower and upper bounds of design variables required for the optimization process can be determined using some preliminary design methods [37]:

$$\begin{aligned} &16.67\ ft \le b \le 39.34\ ft \qquad 30.232\ ft \le b_1 \le 34.166\ ft \qquad 28.413\ ft \le b_3 \le 34.727\ ft \\ &210.6\ ft \le b_4 \le 257.4\ ft \qquad 12.6\ ft \le H_2 \le 15.4\ ft \qquad 302.32\ ft \le H_4 \le 341.66\ ft \\ &270\ ft \le H_5 \le 330\ ft \end{aligned} \tag{43}$$

For design optimization of the selected dam two cases related to various conditions of dam-water-foundation rock interaction problem are considered as follows:

Case 1: Dam with full reservoir and rigid foundation.
Case 2: Dam with full reservoir and flexible foundation.

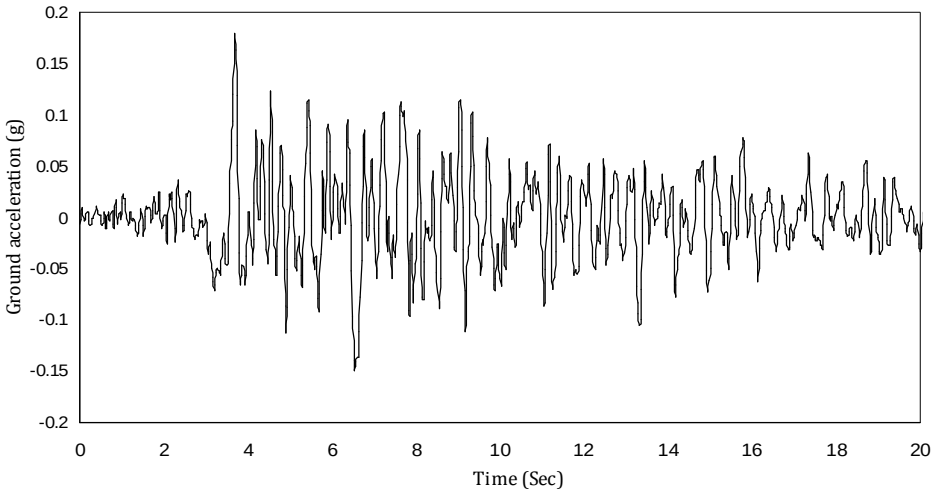

Figure 4. Ground motion at Taft Lincoln Tunnel; Kern country, California, 1952

The parameters of PSO, GSA and GSA-PSO used in optimization process are given in Tables 2, 3 and 4, respectively.

Table 2. The parameter of PSO method

Parameter	Value
Population size	50
Total iteration number	100
$w_{\min}$	0.1
$w_{\max}$	0.9

Table 3. The parameter of GSA method

Parameter	Value
Population size	50
Total iteration number	100
G_0	50.0

Table 4. The parameter of GSA-PSO method

Parameter	Value
The initial number of particles generated via GSA	20
The initial number of particles generated on random basis	30
The maximum number of iterations performing by GSA	50
The maximum number of iterations performing by PSO	50

In this study, the optimization task is performed by a core™2 Duo 2 GHz CPU and all computing times are evaluated by clock time.

7.1. Finite-element model of Pine Flat gravity dam

An idealized model of Pine Flat gravity dam-water-foundation rock system is simulated using FEM as shown in Figure 5. The material properties of the dam, water and foundation rock are given in Table 1. The geometric properties of the dam can be found in Ref. [35].

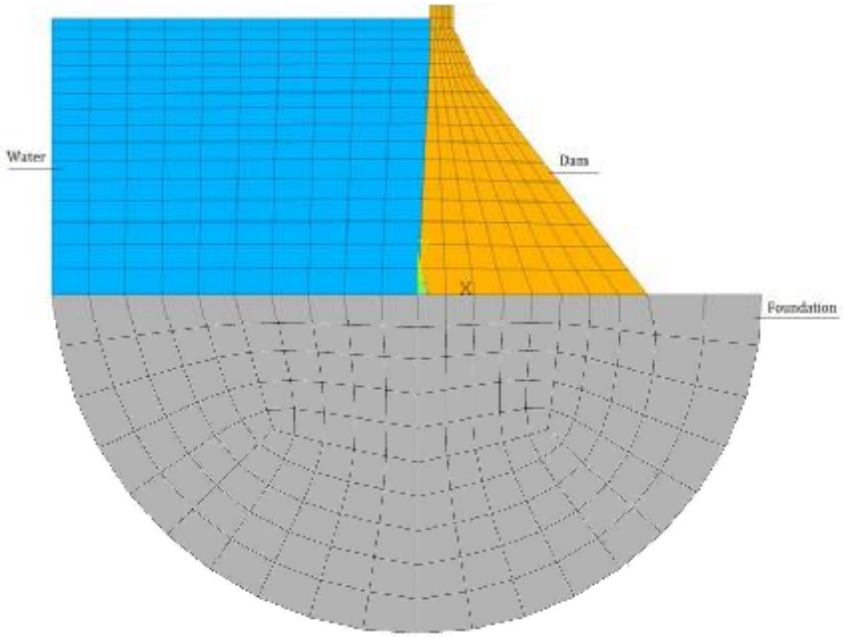

Figure 5. Finite-element model of Pine Flat gravity dam-water-foundation rock system

In order to validate FEM with the employed assumptions, the first natural frequency of the symmetric mode of the gravity dam for four cases are determined from the frequency response function for the crest displacement. The results are compared with those reported by Chopra and Chakrabarti [36] as given in Table 5.

Table 5. A comparison of the natural frequencies from the literature with FEM

Case	Foundation rock condition	Water	Natural frequency (Hz)		
			Chopra and Chakrabarti [36]	The present work	Error (%)
1	Rigid	Empty	3.1546	3.152	0.082
2	Rigid	Full	2.5189	2.525	0.242
3	Flexible	Empty	2.9325	2.93	0.085
4	Flexible	Full	2.3310	2.383	2.18

It can be observed that a good conformity has been achieved between the results of the present work with those reported in the literature.

7.2. Training and testing WLS-SVM

To generate a database for training and testing WLS-SVM, design variable vector of the gravity dam defined in (1) is considered as the input vector of WLS-SVM, and the sum of all active constraints violations given by (19) is taken as the output of WLS-SVM. Design of computer experiments [38] is employed by generating a set of combinations of the intervening design variables. This set is spread in the entire intervening variables by design of computer experiments. In this study, Latin Hypercube Design (LHD) proposed for computer experiments by McKay *et al.* [39] is used for generating 200 gravity dam samples. Then, the effective responses of all gravity dam samples are determined using finite element analysis (FEA). It should be noted that a full dynamic analysis for the design cases 1 and 2 takes about 1.4 and 1.64 minutes, respectively. The samples are selected on a random basis and from which 150 and 50 ones are employed to train and test the performance generality of WLS-SVM.

A mean absolute percentage error, *MAPE*, is used to evaluate the performance of the WLS-SVM model as follows:

$$MAPE = \frac{1}{n_t}\sum_{i=1}^{n_t} 100 \times \left| \frac{y_i - \bar{y}_i}{y_i} \right| \tag{44}$$

where y and $\bar{y}$ are actual value and predicted value, respectively; and n_t is the number of testing samples.

Furthermore, several statistical methods, relative root-mean-squared error, *RRMSE*, and the absolute fraction of variance, R^2, are used to compare predicted and testing values for computing the model validation. The smaller *RRMSE* and *MAPE* and the larger R^2 are indicative of better performance generality. The *RRMSE* and R^2 are defined by using the following equations:

$$RRMSE = \sqrt{\frac{n_t \sum_{i=1}^{n_t} (y_i - \bar{y}_i)^2}{(n_t - 1)\sum_{i=1}^{n_t} y_i^2}} \tag{45}$$

$$R^2 = 1 - \left(\frac{\sum_{i=1}^{n_t} (y_i - \bar{y}_i)^2}{\sum_{i=1}^{n_t} \bar{y}_i^2}\right) \tag{46}$$

In this study, the 10-fold CV is used for finding the parameters and training WLS-SVM. The statistical values and the optimal values of g and s for predicting the effective responses of dam samples found from testing modes are obtained and the results are listed in Table 6.

Table 6. Statistical values based on the optimal values of the WLS-SVM in testing mode

Case	Optimal values		Statistical values		
	g	s	***MAPE***	***RRMSE***	R^2
1	1364.151	80.397	2.4	0.0292	0.9997
2	489.439	32.856	3.62	0.0305	0.9992

All of the statistical values in the table demonstrate that all the WLS-SVM models achieve a good performance generality in predicting the responses of gravity dam samples.

Performance generality of the WLS-SVM in testing mode for two cases are shown in Figures 6 and 7 in term of *APE*.

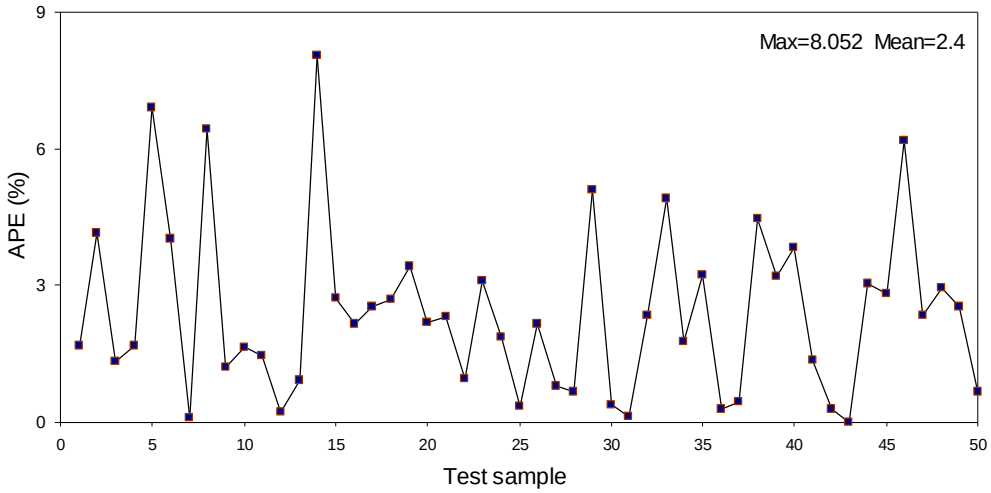

Figure 6. *APE* of the predicted responses for case 1

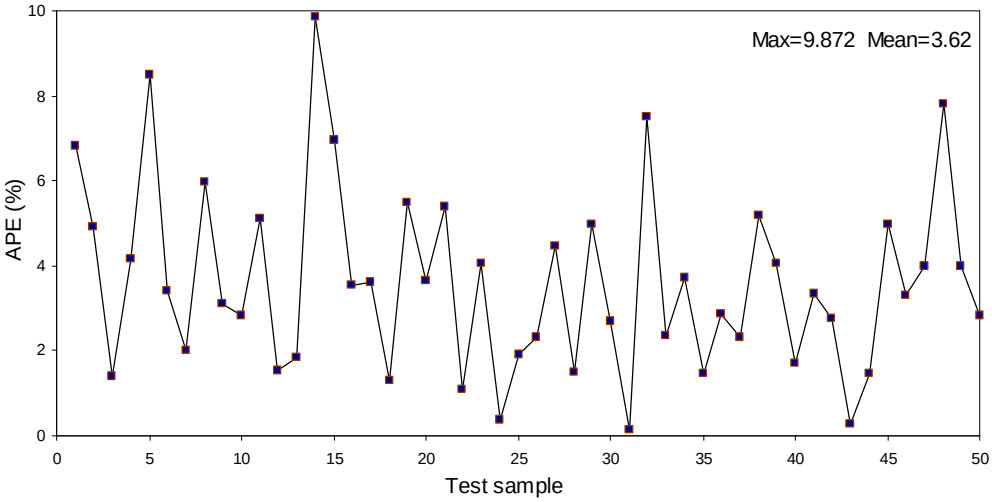

Figure 7. APE of the predicted responses for case 2

7.3. Result of optimization

In order to consider the stochastic nature of the optimization process, ten independent optimization runs are performed for each design case and the best solutions are reported. The optimum designs of the gravity dam for two cases using GSA, PSO and the proposed GSA-PSO based on WLS-SVM as approximate analysis are given in Tables 7 and 8. The convergence histories of the best solutions of PSO, GSA and GSA-PSO for two cases are shown in Figures 8 and 9.

Table 7. Optimum designs of the gravity dam for case 1

Variables	**Optimization Method**		
	PSO	**GSA**	**GSA-PSO**
b (*ft*)	25.3849	21.5092	19.6700
b_1 (*ft*)	31.4449	31.7477	32.0582
b_2 (*ft*)	29.5940	30.1002	29.2068
b_3 (*ft*)	212.4020	219.4519	216.8624
H_2 (*ft*)	15.4000	12.6024	12.6000
H_4 (*ft*)	341.6600	325.4956	331.1774
H_5 (*ft*)	270.0000	270.0000	270.0000
Concrete weight (*kip*)	8309.34	8216.27	8025.79
Maximum violated constraint (%)	0.0	0.0	0.0
Data generation time (min)	279	279	279
Time of training WLS-SVM (min)	1.04	1.04	1.04
Optimization time (min)	0.48	2.69	3.09
Overall computing time (min)	280.52	282.73	283.13
Required approximate analyses	3800	3350	3100

Table 8. Optimum designs of the gravity dam for case 2

Variables	**Optimization Method**		
	PSO	**GSA**	**GSA-PSO**
b (*ft*)	24.6921	26.4482	21.1757
b_1 (*ft*)	31.1698	32.2928	32.2166
b_2 (*ft*)	31.0539	30.6843	30.5364
b_3 (*ft*)	223.7499	226.7058	239.4790
H_2 (*ft*)	15.3994	12.9876	13.7315
H_4 (*ft*)	341.6600	336.7767	337.5632
H_5 (*ft*)	280.5927	270.0000	270.0000
Concrete weight (*kip*)	8777.68	8744.28	8675.56
Maximum violated constraint (%)	0.0	0.0	0.0
Data generation time (min)	327.56	327.56	327.56
Time of training WLS-SVM (min)	1.04	1.04	1.04
Optimization time (min)	0.58	2.77	3.12
Overall computing time (min)	329.18	331.37	331.72
Required approximate analyses	4000	3500	3150

The optimal dams are also analyzed by an accurate FEA and the value of maximum violated constraint for all design cases is determined. The value is zeros for all design cases. Therefore, the optimum solutions are proper designs. The importance of the solutions may be more revealed when a large saving in overall computing time, owing to employing an approximate analysis instead of using a time consuming FEA, is noticed. In GSA-PSO the maximum numbers of searches (i.e. number of approximate structural analyses) for two cases are set equal to 3100 and 3150, respectively. Therefore, the numerical results show that the GSA-PSO converges to superior solutions to GSA and PSO while needing much lower function evaluations.

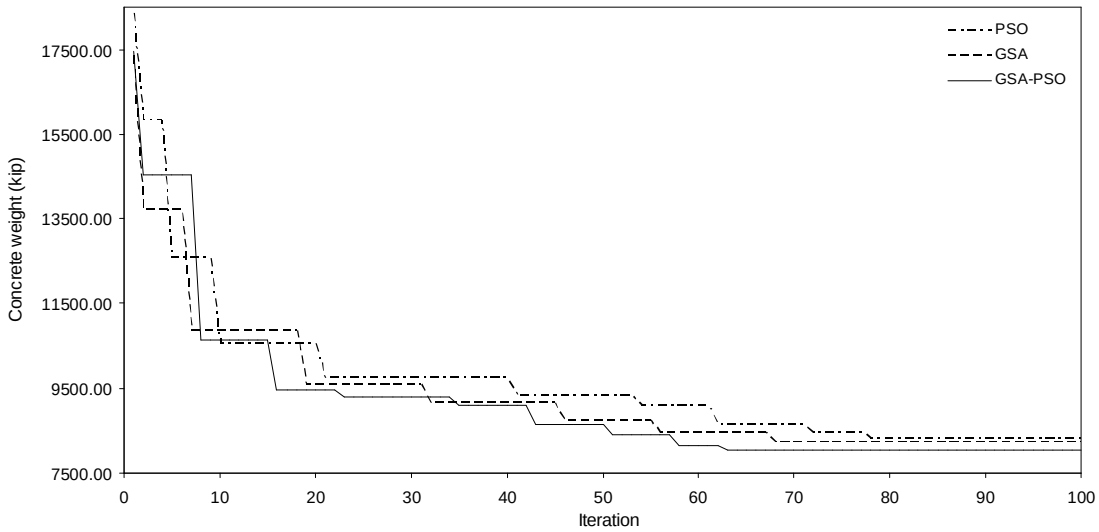

Figure 8. Convergence histories of the best solution of PSO, GSA and GSA-PSO for case 1.

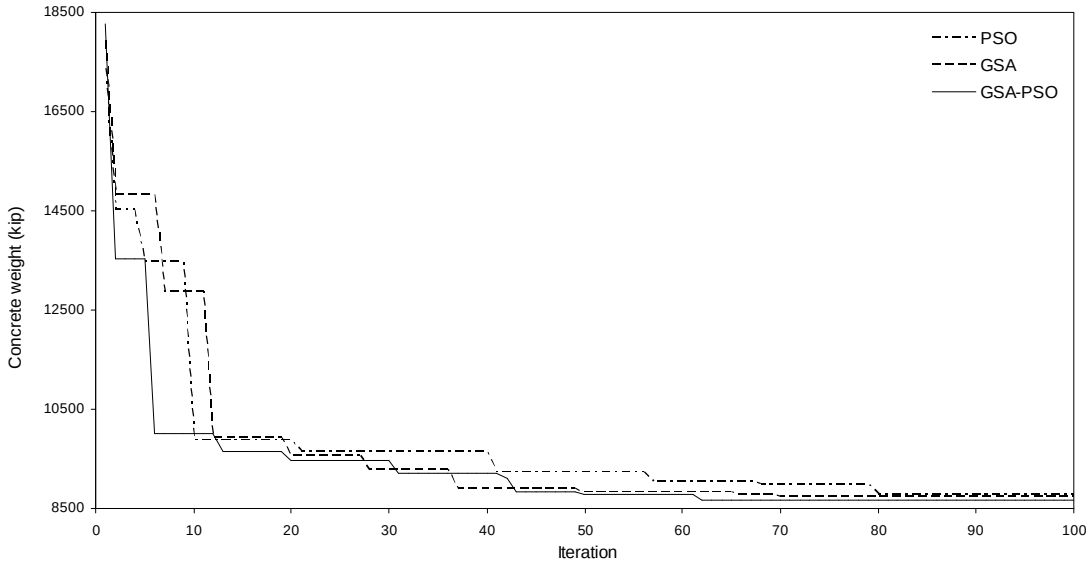

Figure 9. Convergence histories of the best solution of PSO, GSA and GSA-PSO for case 2.

8. CONCLUSIONS

A hybrid meta-heuristic optimization method is developed to find the optimal shapes of concrete gravity dams including dam-water-foundation rock interaction subjected to earthquake loading. The hybrid meta-heuristic optimization method is based on a hybrid of gravitational search algorithm (GSA) and particle swarm optimization (PSO), which is called GSA-PSO. The main idea behind the proposed GSA-PSO is to combine the advantages and avoid the disadvantages of the GSA and PSO methods. Explicitly, GSA-PSO can increase the probability of finding the global optimum while requiring a lower structural analysis. The weighted least squares support vector machine (WLS-SVM) is utilized to approximate the dynamic analysis of the gravity dam instead of directly performing it by a time consuming finite element analysis (FEA). In order to assess the merits of the proposed GSA-PSO and WLS-SVM an existing gravity dam is considered and the optimization is performed for various conditions of the interaction problem. Numerical results show that the proper optimal design can be achieved for the gravity dam. In optimization procedure, FEA is replaced by a WLS-SVM as approximate analysis. The optimum designs obtained by the proposed GSA-PSO are also compared with those produced by GSA and PSO. GSA-PSO shows the improvement in terms of computational efficiency, optimum solution, the number of function measurements and convergence history in the optimization process.

REFERENCES

1. Akbari J, Ahmadi MT, Moharrami H. Advances in concrete arch dams shape optimization, *Appl Math Model* 2011; **35**: 3316-33.
2. William KJ, Warnke ED. *Constitutive model for the triaxial behavior of concrete*, in: Proceedings of International Association for Bridge and Structural Engineering, ISMES, Bergamo, 1975, pp. 1-30.
3. Ricketts RE, Zienkiewicz OC. *Shape Ooptimization of Concrete Ddams, Criteria and Assumptions for Numerical Analysis of Dams*, Quadrant Press, Swansea, London, UK, 1975, pp. 1179-206.
4. Wasserman K, Three dimensional shape optimization of arch dams with prescribed shape function, *J Struct Mech* 1983; **11**: 465-89.
5. Rahim AS. *Optimum Shape of An Arch Dam for Static Loads*, Thesis, Asian Institute of Technology, Bangkok, 1983.
6. Samy MS, Wieland M. Shape optimization of arch dams for static and dynamic loads, in: *Proceedings of International Workshop on Arch Dams*, Coimbra, 1987.
7. Yao TM, Choi KK. Shape optimal design of an arch dam, *J Struct Eng* 1989; **115**: 2401-05.
8. Fanelli A, Fanelli M, Salvaneschi P. A neural network approach to the definition of near optimal arch dam shape, *Dam Eng* 1993; **IV**: 123-40.
9. Maheri M, Bidokhti NT. Shape optimization of concrete arch dams using simple genetic algorithm, *Dam Eng* Xiv, 2001.
10. Salajegheh J, Salajegheh E, Seyedpoor SM, Gholizadeh S. Optimum design of arch dams

including hydrodynamic effects for earthquake loading using the simultaneous perturbation stochastic approximation method, in: *Proceedings of the Ninth International Conference on Computational Structures Technology*, Civil-Comp Press, Stirlingshire, UK, 2008, Paper 60.

11. Seyedpoor SM, Salajegheh J, Salajegheh E, Golizadeh S. Optimum shape design of arch dams for earthquake loading using a fuzzy inference system and wavelet neural networks, *Eng Optim* 2009; **41**: 473-93.
12. Seyedpoor SM, Salajegheh J, Salajegheh E, Golizadeh S. Optimal design of arch dams subjected to earthquake loading by a combination of simultaneous perturbation stochastic approximation and particle swarm algorithms, *Appl Soft Comput* 2011; **11**: 39-48.
13. Akbari J, Ahmadi MT. Shape optimization of concrete arch dams for dynamic loading using mesh design velocity, *Dam Eng* 2009; **XX**: 77-98.
14. Seyedpoor SM, Salajegheh J, Salajegheh E. Shape optimal design of materially nonlinear arch dams including dam-water-foundation rock interaction using an improved PSO algorithm, *Optim Eng*, 2011, 1-22.
15. Chopra AK, Dynamics of Structures: Theory and Applications to Earthquake Engineering. 3rd ed., Prentice Hall, New Jersey, 2006.
16. Kucukarslan S. Dynamic analysis of dam-reservoir foundation interaction in time domain, *Comput Mech* 2004; **33**: 274-81.
17. Kucukarslan S, Coskun B, Taskin B. Transient analysis of dam-reservoir interaction including the reservoir bottom effects, *J Fluids Struct* 2005; **20**: 1073-84.
18. Fenves G, Chopra AK. EAGD-84: A Computer Program for Earthquake Analysis of Concrete Gravity Dams, UCB/EERC-84/11 Report, University of California, Berkeley, USA, 1984.
19. USBR, Design of Gravity Dams, Design manual for Concrete Gravity Dams, U.S. government printing office, 1976.
20. Fourie PC, Groenwold AA. The particle swarm optimization algorithm in size and shape optimization, *Struct Multidisc Optim* 2002; **23**: 259-67.
21. Perez RE, Behdinan K. Particle swarm approach for structural design optimization, *Comput Struct* 2007; **85**: 1579-88.
22. Salajegheh E, Gholizadeh S, Khatibinia M. Optimal design of structures for earthquake loads by a hybrid RBF-BPSO method, *Earthq Eng Eng Vib* 2008; **7**: 14-24.
23. Salajegheh E, Salajegheh J, Seyedpoor SM, Khatibinia M. Optimal design of geometrically nonlinear space trusses using adaptive neuro-fuzzy inference system, *Scientia Iranica* 2009; **6**: 403-14.
24. Kaveh A, Talatahari S. Particle swarm optimizer, ant colony strategy and harmony search scheme hybridized for optimization of truss structures, *Comput Struct* 2009; **87**: 267-83.
25. Gomes HM. Truss optimization with dynamic constraints using a particle swarm algorithm, *Expert Syst Appl* 2011; **38**: 957-68.
26. Fontan M, Ndiaye A, Breysse D, Bos F, Fernandez C. Soil-structure interaction: parameters identification using particle swarm optimization, *Comput Struct* 2011; **89**: 1602-14.
27. Kennedy J, Eberhart RC. *Swarm Intelligence*, Morgan Kaufman Publishers, 2002.
28. Shi Y, Eberhart RC. A Modified Particle Swarm Optimizer in: *Proceedings of IEEE*

International Conference on Evolutionary Computation, IEEE Press, 1998, pp. 69-73.
29. Rashedi E, Nezamabadi-pour H, Saryazdi S. GSA: a gravitational search algorithm, *Inform Sciences* 2009; **179**: 2232-48.
30. Suykens JAK, Brabanter JD, Lukas L, Vandewalle J. Weighted least squares support vector machines: robustness and sparse approximation, *Neurocomputing* 2002; **105**: 85-105.
31. Quan T, Xiaomao Liu X, Liu Q. Weighted least squares support vector machine local region method for nonlinear time series prediction, *Appl Soft Comput* 2010; **10**: 562-6.
32. David HA. Early sample measures of variability, *Stat Sci* 1998; **13**: 368-77.
33. Rousseeuw PJ, Leroy A. *Robust Regression and Outlier Detection*, Wiley-Interscience, New York, 1987.
34. Cawley GC. Leave-one-out cross-validation based model selection criteria for weighted LS-SVM, in: *Proceedings of the International Joint Conference on Neural Networks*, Vancouver, BC, Canada, 2006, pp. 1661-1668.
35. Vargas-Loli L, Fenves G. Effects of concrete cracking of the earthquake response of gravity dams, *Earthquake Eng Struct Dyn* 1989; **18**: 575-92.
36. Chopra AK, Chakrabarti P. *Earthquake Response of Concrete Gravity Dams Including Hydrodynamic Foundation Interaction Effects*, UCB/EERC-80/01 Report. University of California, Berkeley, USA, 1980.
37. Varshney RS. *Concrete Dams*, Oxford and IBH Publishing Co, New Delhi, 1982.
38. Fang KT, Li R, Sudjianto A. *Design and Modelling for Computer Experiments*, CRC Press, New York, 2006.
39. Mckay MD, Beckman RJ, Conover WJ. A comparison of three methods for selecting values on input variables in the analysis of output from a computer code, *Technometrics*, 1979; **21**: 439-45.